Submitted, accepted and published by
Energy & Fuels 2011, 25, 1316-1326

Effect of support on the behaviour of Cu-based oxygen carriers during long-term CLC operation at temperatures above 1073 K

Pilar Gayán [1], Carmen R. Forero [2], Alberto Abad [1], Luis F. de Diego [1], Francisco García-Labiano [1] and Juan Adánez.[1]*

1 Instituto de Carboquímica (CSIC), Dept. of Energy & Environment, Miguel Luesma Castán, 4, Zaragoza, 50018, Spain.

2 University of Valle, Engineering School of Natural and Environmental Resources (EIDENAR). Calle 13 No. 100-00, 25360 Cali, Colombia, e-mail: caforero@univalle.edu.co. Fax: (+34) 976 733 318.

* Corresponding author: Tel: (+34) 976 733 977. Fax: (+34) 976 733 318. E-mail address: pgayan@icb.csic.es (Pilar Gayán Sanz)

Abstract

Chemical-Looping Combustion (CLC) is a combustion technology with CO_2 capture that is characterized by its low energy penalties because the CO_2 separation is inherent to the process. The CLC concept is based on the transfer of oxygen from the combustion air to fuel by means of an oxygen carrier (OC) in the form of a metal oxide. The OC circulates

between two interconnected reactors, the fuel (FR) and the air reactor (AR). To scale up the CLC process for industrial application OCs materials suitable to work at high temperatures are needed. Cu-based OCs had been proved to fulfil the requirements for an OC material, although operating temperatures lower than 1073 K has been recommended due to its likely agglomeration problems. In this work, several Cu-based OCs have been developed by impregnation on different supports. The supports were prepared by thermal or chemical modifications of commercial γAl_2O_3 with the aim of reduce the interaction with the metal oxide. The behaviour of the OCs was studied in a CLC continuous unit of 500 W_{th} during long-term tests using methane as fuel gas and high operation temperatures (1173K in the FR and 1223 K in the AR). The effect of the high FR and AR temperatures on the process performance was evaluated taking into account important aspects such as combustion efficiency, resistance to attrition, fluidization behaviour (no presence of agglomeration) and maintenance of the oxygen transport capacity and reactivity. Agglomeration or deactivation of the particles was never detected with neither of the oxygen carriers used. At these high temperatures, stable operation for more than 67 h was feasible only using an oxygen carrier with γAl_2O_3 modified with NiO addition as support. This is the first time that a Cu-based OC, prepared by a commercial manufacturing method, and used at 1173K in the FR and 1223 K in the AR exhibits such a good properties: high reactivity together with high mechanical durability and absence of agglomeration. This result opens new possibilities for the application of Cu-based materials in industrial-scale CLC processes.

Keywords: CO_2 capture, chemical-looping combustion, copper.

1. Introduction

In order to stabilize the CO_2 concentration in the atmosphere, several measures must be taken. In most scenarios for the stabilization of atmospheric greenhouse gas concentrations between 450 and 750ppmv CO_2, the Carbon Capture and Storage (CCS) will contribute 15–55% to the cumulative mitigation effort worldwide until 2100 [1] . The CCS is a process involving the separation of CO_2 emitted by industry and energy-related sources, and the storage for its isolation from the atmosphere over the long term. Chemical Looping Combustion (CLC) process has been suggested among the best alternatives to reduce the economic cost of CO_2 capture using fuel gas [2] and to increase the efficiency with respect to other CO_2 capture process [3]. In this process, CO_2 is inherently separated from other combustion products, N_2 and unused O_2, through the use of a solid oxygen carrier (OC) and thus no energy is expended for the separation.

The CLC process has been demonstrated for gaseous fuels such as methane or natural gas in 10-140 kW_{th} units using Ni or Cu-based oxygen carriers [4-8] and for syngas combustion using Co, Ni or ilmenite as oxygen carriers [9].

A cornerstone in the successful development of a CLC system is the OC, which is composed of a metal oxide and a support. The OC besides having a high reactivity with the gas fuel and air during many cycles of reduction-oxidation and full fuel conversion to

CO_2 and H_2O, must meet other characteristics such as low attrition, no agglomeration during fluidized bed operation, and no carbon deposition. Among the different metal oxides proposed in the literature for the CLC process, Cu-based oxygen carriers have shown high reaction rates and oxygen transfer capacity [10], and have no thermodynamic restrictions for complete fuel conversion to CO_2 and H_2O. In addition, the use of Cu-based oxygen carriers has less environmental problems and costs than other materials used for CLC process such as nickel, cobalt, etc.

Several Cu-based OC has been developed using different supports and preparation methods [10-14]. Our research group at the Instituto of Carboquímica (CSIC) has undertaken several studies using oxygen carriers based on copper. Potential Cu-based oxygen carriers were prepared using different supports [10]. It was found that the optimum preparation method for Cu-based oxygen carriers was the impregnation on a support [15]. Later, the preparation conditions and oxygen carrier characteristics were optimized to avoid the agglomeration of the Cu-based materials during their operation in a fluidized bed [16]. Based on these findings, a Cu-based oxygen carrier support on γ-Al_2O_3 was finally selected to test its behaviour during 200 h of continuous operation in a 10 kW_{th} CLC prototype using methane as fuel at 1073 K in both FR and AR [6]. A waste management study using Cu-based materials coming from this CLC plant concluded that the solid residues generated in a CLC plant using Cu-based materials can be classified as a stable non-reactive hazardous waste, acceptable at landfills for non-hazardous wastes [17]. Additional work has been recently carried out to test the behaviour of this oxygen carrier in a CLC continuous unit of 500 W_{th} using syngas as fuel [18] or methane containing

variable amounts of light hydrocarbons (LHC) or H_2S [19, 20]. It was found that the OC can fully convert syngas or methane at 1073 K and no special measures should be adopted due to the presence of LHC in the fuel gas. With respect to the presence of H_2S in the fuel gas,it was found that the great majority of the sulphur fed into the system was released in the gas outlet of the FR as SO_2, affecting only to the quality of the CO_2 produced.

To summarized, Cu-based oxygen carrier supported on γ-Al_2O_3 had been proved to fulfil the requirements for an OC material, although operational temperatures lower than 1073 K were always used in the FR. This temperature was recommended to avoid agglomeration problems derived from the use of temperatures near to the melting point of metal, 1358K for metallic Cu. However, an increase in the operation temperature would increase the efficiency of the whole process.

There is a concern about how to integrate the CLC process in a power plant maximizing the net efficiency [21-25]. Naqvi and Bolland, (2007) proposed a CLC combined cycle with a 45.1 % of net plant efficiency at 1173 K with close to 100 % of CO_2 capture. It is well known that in a thermal process, increasing the inlet gas temperature in the gas turbine increases the net efficiency of the process. An increase of 200 K in this temperature could cause an increase in the net plant efficiency until values about 49.7 %. However, these authors proposed a CLC combined with reheat in the air turbine at relatively low and safe oxidation temperature (1173 K) resulting in a 49% of net plant efficiency. This efficiency is higher than conventional combined cycle with 90% of CO_2 capture (48.6%).

To scale up the CLC technology information about the high temperature resistance of the oxygen carriers is needed. By temperature resistance is meant the ability to withstand high temperature without defluidizing or agglomerating, with low attrition rate and stable reactivity. Agglomeration problems are particularly important working with Cu-based OC as it was pointed out before [11, 26] due to the low melting temperature of the metallic Cu. In addition, the attrition rate of the oxygen carriers is another important parameter to be accounted as a criterion for using a specific material in a fluidized bed reactor. High attrition rates will decrease the lifetime of the particles increasing the cost of the CLC process.

There are in the literature very few works dealing with the temperature resistance of the Cu-based OC. de Diego et al., (2005) used a CuO/γ-Al_2O_3 oxygen carrier at 1223 K in a batch fluidized bed reactor during 20 reduction and oxidation cycles. They found that the behaviour of the oxygen carrier with respect to chemical stability and reactivity was satisfactory despite the high temperature used, although a small number of cycles were carried out. Very recently, [27] have analyzed the behaviour of this CuO/γ-Al_2O_3 oxygen carrier during long-term tests at FR temperatures up to 1173 K and AR temperatures up to 1223 K under continuous operation in a CLC unit 500 W_{th}. They found that both T_{FR} and T_{AR} had a great influence on the resistance to attrition of the particles. Stable operation for more than 60 h was feasible at T_{FR} =1073 K and T_{AR} = 1173 K without agglomeration problems or deactivation of the carrier. However, an increase of 100 K in the AR temperature operation produced a reduction in the particle lifetime from 2700 to

1100 h. It was indicated that a support with a minimized interaction with the metal oxide might be useful to increase the temperature resistance of copper-based oxygen carriers.

It is well known that the support has a great influence on the behaviour of the oxygen carriers [10, 15, 28]. de Diego et al. (2005) and Gayán et al. (2008) found that an increase in the calcination temperature of an γ-alumina support produced a decrease on the attrition rate due to the phase transformation of γ-Al_2O_3 to α-Al_2O_3, a more stable phase. Moreover, $MgAl_2O_4$ offer a desirable combination of properties like high melting point, high resistance to chemical attack, and high strength at elevated temperatures [29] and it has been used as support for oxygen carriers with satisfactory results [28, 30]. On the other hand, Adánez et al., 2006 [31] studied the behaviour of different Ni-Cu oxygen carriers using alumina as support in a batch fluidized bed working at 1123K. They found that to have a stable and low attrition rate at high temperature was necessary the existence of a minimum amount of NiO (about 4 wt. %) in the oxygen carrier to stabilize the CuO phase.

In this paper, several Cu-based oxygen carriers were prepared by incipient wet impregnation using different supports. Various routes to minimize the CuO interaction with the support were studied using commercial γ-alumina as material support and introducing modifications via thermal or chemical pre-treatment with Mg or Ni oxides. The influence of the support on the high temperature behaviour of the different Cu-based oxygen carriers was analyzed during long-term test in a 500 W_{th} CLC unit under continuous operation using methane as fuel and high temperatures both in FR, 1173 K

and in AR, 1223 K. The influence of the support on the combustion efficiency, attrition rate and material agglomeration was investigated. Changes in particles with respect to reactivity, chemical composition and physical characteristic were also analyzed. According to a literature review, this is the first time that the performance of different Cu-based oxygen carriers was evaluated during long-term test at so high temperatures.

2. Experimental

2.1. Preparation of oxygen carrier

Different oxygen carriers were prepared by incipient wet impregnation method using CuO as active phase and γ-Al_2O_3, α-Al_2O_3, $MgAl_2O_4$, and NiO/γ-Al_2O_3 as supports.

Supports. Commercial γ-Al_2O_3 particles (Puralox NWa-155, Sasol Germany GmbH) of 300-500 μm with a density of 1.3 g/cm^3 and a porosity of 55.4% was used as raw material to prepare the different supports. Thermal or chemical pre-treatment of this γ-Al_2O_3 were used in the preparation of the modified supports. The thermal treatment was carried out by sintering the γ-Al_2O_3 in a furnace at 1423 K during 2 h. An α-Al_2O_3 support with a density of 2 g/cm^3 and a porosity of 47.3% was obtained.

The chemical pre-treatment consisted in precoating the support with MgO or NiO. $MgAl_2O_4$ as support was obtained by incipient wet impregnation on γ-Al_2O_3 with $Mg(NO_3)_2.6H_2O$ (>99.5 % Panreac) solution. The corresponding MgO content (27 wt.%) was achieved by applying successive impregnations followed by calcination at 823 K in air atmosphere for 1 h to decompose the impregnated nitrate. Finally, the support

was stabilized in air atmosphere at 1073 K during 1 h to obtain a support with complete conversion of alumina into $MgAl_2O_4$. The $NiO/\gamma\text{-}Al_2O_3$ support was obtained by incipient wet impregnation on $\gamma\text{-}Al_2O_3$ with $Ni(NO_3)_2.6H_2O$ (>99.5 % Panreac) solution followed by calcination at 823 K to obtain a support with 3 wt.% of NiO.

Oxygen carriers. Cu-based OCs were prepared by the addition of a volume of saturated copper nitrate solution corresponding to the total pore volume of the support particles. The aqueous solution was slowly added to the support particles, with thorough stirring at room temperature. The desired active phase loading was achieved by applying successive impregnations followed by calcination at 823 K, in air atmosphere for 30 min in a muffle oven to decompose the impregnated copper nitrate into copper oxide. Finally, the oxygen carrier was stabilized in air atmosphere for 1 hour at 1123 K. The main characteristics of the Cu-based oxygen carriers are showed in Table 1. The different OCs were named as Cu-γAl, Cu-αAl, Cu-MgAl and Cu-NiAl, according to the support used in the preparation.

2.2. Oxygen carriers characterization

Fresh and after-used samples of the oxygen carriers were physically and chemically characterized by several techniques. The reactivity of the OC was determined by TGA techniques using CH_4 as fuel [32]. The oxygen transport capacity, defined as the mass fraction of oxygen that can be used for the oxygen transfer, was determined by thermogravimetric analysis using H_2 as fuel. This property is calculated as $R_{o,OC} = (m_{ox}$ -

$m_{red})/m_{ox}$, where m_{ox} and m_{red} are the weights of the oxidized and reduced forms of the oxygen carrier, respectively. The determination of particle size diameter (PSD) was made with a LS 13 320 of Beckman Coulter equipment. The system allows the PSD determination ranging from 0.04 to 2000 microns. The bulk density of the oxygen carrier particles was calculated weighting a known volume of solid and assuming that the void was 0.45 corresponding to loosely packed bed. The specific surface area was estimating by the Brunauer-Emmett-Teller (BET) method using a Micromeritics ASAP 2020. The porosity was measured by Hg intrusion in a Quantachrome PoreMaster 33. The force needed to fracture a particle was determined using a Shimpo FGN-5X crushing strength apparatus. The crushing strength was taken as the average value of at least of 20 measurements. The identification of crystalline chemical species was carried out by powder X-Ray Diffraction (XRD) in a Bruker AXS D8 Advance, equipped with monochromatic beam diffracted graphite, using Ni-filtered "Cu Kα" radiation. Temperature-programmed reduction (TPR) studies were performed in an AutoChem II Micromeritics equipment, using 150 mg of sample. Each sample was heated in a 10% H_2/Ar flow (50 cm^3/min) from 323 K to 1323 K at 10 K/min. TPR analysis was used to provide information on the reducibility species of the carrier. The microstructures of the particles and element distribution in the solid were observed by a Scanning Electron Microscopy (SEM) in a Hitachi S-3400 N, with an Energy Dispersive X-Ray (EDX) analyzer Röntec XFlash of Si(Li). To analyze the internal section of the particles, some particles were embedded in resin, cut with a diamond blade and polished.

2.3. CLC continuous unit of 500 W_{th}

Figure 1 show a schematic diagram of the reactor system, located at "Instituto de Carboquímica" (CSIC). The facility used in this study is a CLC continuous unit of 500 W_{th} composed of two interconnected fluidized bed reactors. Detailed information about the prototype and operating procedure used can be found elsewhere [18].

The fuel reactor (A) and the air reactor (C) are separated by a loop seal (B) to avoid mixing fuel and air. The solids from the AR are transported by a riser (D), recovered by a cyclone (E) and returned to the FR trough a solids valve (G) that controls the solid circulation rate and also acts as a loop seal. The diverting solids valve (H) can measure this circulation rate. Moreover, the composition of both outlet streams is analyzed using on-line specific gas analyzers. Fine particles produced by attrition were recovered in the filters placed downstream of both reactors. The prototype allowed the collection of solid material samples from the AR at any moment from the diverting solid valve (H), and from the FR at the end of the test.

The solid inventory in the plant was about of 1.2 kg of OC. The inlet gas flow in the FR was 260 lN/h corresponding a gas velocity of 0.14 m/s, which was about 2.5 times the minimum fluidization velocity of the particles. The fuel gas in the FR was methane diluted in nitrogen. Nitrogen was used as a fluidizing agent in the bottom loop seal (45 lN/h). Air was used as fluidizing gas in the AR. To achieve complete oxidation of the reduced oxygen carrier in the AR, the air was divided into the fluidizing gas in the

bottom bed (720 lN/h), allowing high residence times of the particles, and into the secondary air in the riser (150 lN/h) to help particle entrainment.

2.3.1. Combustion tests

Long-term CLC tests under different operating conditions were carried out at high temperature both in the FR (T_{FR} = 1173 K) as in the AR (T_{AR} = 1223 K) using Cu-based oxygen carriers and methane as fuel. Table 2 shows a summary of the operating conditions used in each test. FR and AR temperatures were kept constant during overall operation for each test using the same batch of oxygen carrier particles. The duration of the tests were fixed to be long enough to analyze the effect of temperature on the physical and chemical characteristics of the particles and make a reliable estimation of the particle lifetime at those conditions. Some tests should be early stopped due to operational problems caused by the amount of fines generated. More than 50 h in hot conditions were carried out in those tests where operation of the plant was possible. A total of about of 209 h at hot condition in the CLC continuous unit 500 kW_{th} were carried out in this work, of which 176 h corresponded at combustion conditions with methane.

Moreover, the effect of the operating conditions on the combustion efficiency was also analysed in each test. Thus, the effect of the oxygen carrier to fuel ratio, ϕ, on the combustion efficiency was carried out varying the fuel concentration but keeping all the other experimental conditions constant. It must be pointed out, that although during the first 10 h of operation the experiments were carried out at different power inputs, the

solids inventory in the FR (≈ 0.2 kg) and the air flow in the AR were maintained constant. The remaining operation time was carried out at constant operating conditions corresponding to those of complete combustion of methane.

Air flow into the AR was maintained constant for all tests remaining always in excess over the stoichiometric oxygen demanded by the fuel gas. The air ratio, λ defined in Eq. (1), ranged from 1.0 to 1.5 depending on the fuel flow.

$$\lambda = \frac{\text{Oxygen flow}}{\text{Oxygen demand}} = \frac{0.21 F_{air}}{2 F_{CH4}} \qquad (1)$$

The combustion efficiency was defined as the ratio of the oxygen consumed by the gas leaving the FR to that consumed by the gas when the fuel is completely burnt to CO_2 and H_2O. So, the ratio gives an idea about how the CLC operation is close or far from the full combustion of the fuel, i.e. $\eta_c = 100\%$.

$$\eta_C = \frac{\left(2x_{CO_2} + x_{CO} + x_{H_2O}\right)_{out} F_{out}}{\left(4x_{CH4}\right)_{in} F_{in}} 100 \quad (2)$$

where F_{in} is the molar flow of the inlet gas stream, F_{out} is the molar flow of the outlet gas stream, and x_i is the molar fraction of the gas i corresponding to the inlet or outlet.

The oxygen carrier to fuel ratio (ϕ) was defined by Eq. (3), where F_{CuO} is the molar flow rate of the copper oxide and F_{CH_4} is the inlet molar flow rate of the CH_4 in the FR. A value of ϕ = 1 corresponds to the stoichiometric CuO amount needed for a full conversion of the fuel to CO_2 and H_2O:

$$\phi = \frac{F_{CuO}}{4\,F_{CH_4}} \quad (3)$$

3. Results and discussion

The four different Cu-based oxygen carriers have been tested in a CLC continuous unit of 500 W_{th} at high temperatures using methane as fuel during long-term tests. The results are presented analyzing the influence of the FR and AR temperatures and oxygen carrier to fuel ratio on the combustion efficiency and on the behaviour of the OC with respect to material agglomeration, attrition rate and particle integrity with the different OCs.

3.1. Combustion efficiency

To analyze the behaviour of the different Cu-based oxygen carriers during methane combustion at high temperature, several tests under continuous operation were carried out at different ϕ values (see Table 2). The steady-state for the different operating conditions was maintained at least for two hours in each test.

Fig. 2 shows the effect of the oxygen carrier to fuel ratio, ϕ, on the combustion efficiency at T_{FR} = 1173 K and T_{AR} = 1223 K with the different OCs. In all cases an increase in ϕ produces an increase in the combustion efficiency. All Cu-based OCs achieved full conversion of methane at low ϕ values (ϕ > 1.2). This result showed the high reactivity of all OCs, independently of the support used.

3.2. Oxygen carrier behaviour

Besides full combustion, other aspects like agglomeration, attrition, reactivity, and oxygen carrier properties should be considered to evaluate the behaviour of the different oxygen carriers during tests at high temperature.

3.2.1. Agglomeration

As discussed above, the oxygen carriers based on copper have been rejected as candidates for the CLC system because could present agglomeration problems [11, 26]. Despite this background, de Diego et al. (2005) found suitable preparation conditions to avoid this phenomenon and thus take benefit of its main advantages: high oxygen transport capacity and reactivity, complete combustion to CO_2 and H_2O without producing CO or H_2, exothermic reactions both in oxidation and in reduction, together with a moderate cost and low toxicity.

The Cu-based OCs used in this work were manufactured following the preparation conditions that avoid agglomeration problems indicated by de Diego et al., 2005, that is, low CuO content (< 20 %) and low calcination temperature (< 1123 K). Agglomeration problems in the CLC continuous unit can be detected by pressure drop measurements. If agglomeration occurred, the gas flow passed through preferential pathways drastically decreasing the bed pressure drop, and reducing the amount of active oxygen-carrier material. However, in spite of that the high operation temperatures used in the experiments, agglomeration or defluidization of the reactors (FR or AR) were never detected. SEM micrographs of used samples extracted at the end of the experiments from both FR and AR for the different OCs confirmed that individual particles maintained their original shape without formation of bridges between particles. Figure 3 shows that no substantial morphological changes were detected and particles remained independent. These results are very relevant for the future use of Cu-based materials as oxygen carrier for CLC technology taking into account the high temperatures used in the tests (T_{FR} = 1173 K, and T_{AR} = 1223 K).

3.2.2. Attrition rates

Attrition and/or fragmentation of particles were analyzed during continuous long-term tests at high temperature. Abrasive attrition and fines generated from the fragmentation of particles are two possible mechanisms of fines generation that can occur in fluidised beds. The occurrence of fragmentation can be deduced from changes in the particle size distribution (PSD) of the samples recovered from the CLC system during each long-term

test. The particle size distribution of both fresh and extracted particles from the reactors at the end of the test for each oxygen carrier were compared. It was found that all used particles do not exhibit much evidence of fragmentation, thereby indicating that fines are generated primarily by abrasive attrition.

Particles elutriated from the fluidized bed reactors during operation were recovered in the filters and weighted to determine the attrition rate. The loss of fines was defined as the loss of particles smaller than 40 μm [33]. Particles of sizes > 40 μm recovered in the filters were recycled into the system.

Attrition rate (A), was defined by Eq. (4), where w_f is the weight of elutriated particles < 40 μm during a period of time, w_t is the weight of total solids inventory and Δt is a period of time during the particles were collected.

$$A = \frac{w_f}{w_t . \Delta t} 100 \qquad (4)$$

Attrition rate is a useful measure to estimate the lifetime of particles. Fig. 4 shows the evolution with time of the attrition rate during the operation in the CLC continuous unit of 500 W_{th} with the different OCs. The generation of fine particles was high at the beginning of the operation for the OCs prepared using γ-alumina (Cu-γAl), $MgAl_2O_4$ (Cu-MgAl) and $NiO/\gamma Al_2O_3$ (Cu-NiAl), due to the rounding effects on the irregularities of the particles and fines stuck to the particles during preparation. The OC prepared using α-alumina as support (Cu-αAl) has a very low initial attrition rate. This can be due

that this OC has the highest crushing strength (see Table 1) due to the thermal treatment at high temperature during support preparation. Later, the attrition rate due to the internal changes produced in the particles by the successive reduction and oxidation cycles during operation at high temperatures (T_{FR} = 1173 K and T_{AR} = 1223 K) presented different behaviour depending on the OC.

The Cu-γAl and Cu-αAl OCs presented an abrupt increase of the generation of fines after 20 h of operation resembling that the particles had chunked. The amount of fines was too high and forced to stop operation in the plant. The Cu-MgAl OC had a stable attrition rate, although with a high value (0.2 wt. % / h) corresponding to a particle lifetime of 500 h. It can be seen from Fig. 4 that only with Cu-NiAl OC the system was running satisfactorily around 67 h, with a stable and low value of the attrition rate (0.04 %), giving an estimation of the particle lifetime around 2700 h. This value is comparable to the one calculated for a CuO-γAl_2O_3 oxygen carrier during 100 h of operation in a 10 kW CLC pilot plant, although working at lower temperatures (1073 K) in both reactors [34]. As it can be inferred from these results, an increase of 100 K in the T_{FR} and 150 K in T_{AR} can be done without a detrimental effect on the particle lifetime. The reasons of the high attrition rates obtained with the OCs prepared on γ-alumina, α-alumina, and $MgAl_2O_4$ as supports will be discussed later.

3.2.3. Reactivity

Since in every cycle of CLC process the oxygen carrier undergoes important chemical and structural changes at high temperature, substantial changes in the reactivity with the number of cycles might be expected. The CuO content in the particles recovered in the filters and in the different samples taken at the outlet of the AR during operation was determined in TGA using H_2 as reduction gas. The CuO content in the particles recovered in the filters was significantly higher than that in the corresponding fresh oxygen carrier particles. On the other hand, the CuO content of the samples taken at the outlet of the AR decreased as the operation time increased for all the OCs used. Table 3 shows the final CuO content measured in samples extracted from the AR at the end of the test for each OC. Figure 5 shows the evolution with time of the CuO content of the samples extracted from the AR during operation at high temperature for the different OCs. As can be observed, a decrease in the final value of the CuO content was obtained for all the different OCs. At the beginning, the CuO content sharply decreased for all samples; however, after 15 h of operation, the CuO content of the oxygen carriers decreased until a relatively constant value for the rest of the operation time. It must be pointed out the important decrease in the CuO content measured with the Cu-MgAl OC. In a previous work, Adánez et al. (2006) using CuO-γAl_2O_3 particles in a 10 kW_{th} unit operated at lower temperatures (T_{FR} = 1073 K and T_{AR} = 1073 K) measured a loss of CuO content in the particles taken at the outlet of the AR as the operational time increased. The results found in this work agreed with those found by Adánez et al. (2006), which attributed the copper lost to the erosion of the CuO grains present in the external surface of the fresh particles. Similar reason can be adduced here.

The CuO content reduction measured for all OCs during the operation in the CLC plant produced a decrease in the oxygen transport capacity of the OCs and might be changes in the reactivity. However, in spite of the reduction in the oxygen transport capacity, full combustion efficiency for $\phi > 1.2$ were always reached in the CLC continuous unit during operation. Figure 6 shows the conversion curves obtained in TGA at 1073 K, using a mixture of 15 vol %CH_4, 20 vol % H_2O, and 65 vol % N_2 in the fresh oxygen carrier and in samples taken at the end of the different tests, corresponding also to different operation times. Some differences in the reduction reactivities were observed depending on the support used. After-used Cu-γAl and Cu-αAl OCs maintained their high reactivity. Cu-MgAl and Cu-NiAl OCs presented a decrease in the reduction reactivity, being more significant for Cu-MgAl OC. This fact could be due to the great copper sintering process that these particles experienced after being used at high temperature, as was corroborated by SEM. However, in all cases, the used particles were fully reduced below 60 s, and showed very high oxidation reactivities, indicating that particles maintain its high reactivity after operation at high temperatures in the CLC unit.

3.2.4. Characterization of Cu-based oxygen carriers

To analyze the results obtained regarding the effect of FR and AR temperatures on the behaviour of the particles, physical and chemical properties of the oxygen carrier particles coming from the AR, and from fines recovered in the filters at the FR and AR outlet streams were compared to those of fresh particles. Table 3 shows the main

properties of the different materials after used in the CLC continuous unit of 500 W_{th} during long-term tests.

Porosity. Figure 7 shows the pore size distribution of the fresh and after used oxygen carriers at the end of the test. It can be seen in fresh OCs that the thermal pre-treatment of the γAl_2O_3 to produce αAl_2O_3 increase the mean pore size from ~12 nm to ~100 nm, decreasing the porosity and the specific surface area of the corresponding OC (see Table 1). The chemical pre-treatment of the γAl_2O_3 to produce $MgAl_2O_4$ (27 %) and $NiOAl_2O_4$ (6 %) hardly affected the pore size distribution of γAl_2O_3. However, the value of the porosity and specific surface area decreased in the case of Cu-MgAl due to the several numbers of calcinations required to produce this OC. At the end of the tests, the pore size distribution of the different samples had changed considerably with respect to the fresh particles with the full disappearance of 12 nm pores. The mean pore size shifted towards pores of higher size, indicating the presence of macro pores inside the particles. The major change in porosity (from 50 % to 58 %) corresponds to the Cu-γAl OC. Changes in porosity are related with changes in the oxygen carrier bulk density, consequently the majority of the OCs presented a minor decrease of this characteristic.

Specific surface area. Fresh Cu-αAl OC had a very low specific surface area compared to the other fresh OCs. This decreased is associated with the formation of α-Al_2O_3 during the calcination process of the γ-Al_2O_3.

The BET specific surface area of all used OCs decreased. The decrease for Cu-γAl, Cu-MgAl, and Cu-NiAl OCs was due to that thermal sintering occurred inside the particles due to the high operational temperatures used in FR and AR.

Crushing strength. The evolution with time of the crushing strength of the different OCs particles at high operation temperature was measured from samples extracted from the AR. Figure 8 shows the effect of the support on the crushing strength at different operation times. The fresh OCs had notably different crushing strength, being the corresponding to CuO-αAl_2O_3 the highest and two times than the corresponding to Cu-MgAl. It can be seen that the support used to prepare the different OCs had an important effect on the crushing strength evolution of the particles. Cu-γAl and Cu-αAl presented a fast and important decrease of this property, with a value of less than 1N for the Cu-γAl OC after 25 h of operation. However, Cu-MgAl, and Cu-NiAl OCs had a smooth decrease, with a value of 1.7 N and 2.1 N respectively at the end of operation at high temperature. Although the relation between crushing strength and particle lifetime is not well established, it is believed that values considerably lower than 1N might be too soft for long-time circulation [35]. Moreover, although fresh CuO-αAl_2O_3 particles had the highest crushing strength of the different OCs (4.6 N), the attrition rate measured in the long term test was very high and operation was stopped after 30 h. Therefore, the initial values of the crushing strength of the OC particles are not a suitable characteristic to evaluate the particle lifetime in the process. As it was found in this work, the support used in the OC manufacture strongly affects to the fluidization behaviour of the OC.

Crystalline phases. Powder XRD patterns of the fresh carriers, shown in Table 1, revealed the presence of CuO, and the corresponding support (γ-Al_2O_3 or α-Al_2O_3 and $MgAl_2O_4$) as the main crystalline phases for fresh OCs. The interaction of copper with the support is revealed through the formation of copper aluminate, $CuAl_2O_4$, in Cu-γAl, Cu-αAl, and Cu-NiAl OCs. $MgAl_2O_4$ and $NiAl_2O_4$ are also present in the corresponding OCs.

Powder XRD analysis of samples extracted from the AR and collected at the outlet of the AR and FR streams at the end of each long-term test are also showed in Table 3. The powder XRD patterns of the used samples revealed the transformation of the γ-Al_2O_3 to α-Al_2O_3 in both Cu-γAl and Cu-NiAl OCs as a most stable phase at high temperature, explaining the observed evolution of the textural properties of the used particles. A new copper aluminate, $CuAlO_2$, was detected in used particles of Cu-γAl and Cu-αAl. Reduced CuO phases, Cu_2O and Cu, were detected in all the samples collected in the filter at the outlet of the FR. Oxidized compounds of copper (CuO and copper aluminates) were only found in the samples coming from the AR and from the AR filter, verifying that the oxygen carrier reached always full oxidation state in the AR.

The XRD spectra of Cu-MgAl OC revealed that some MgO compound is present in the used samples extracted from the AR. MgO may be formed by the following solid state reaction favoured at temperatures around 1273 K [36]:

$$MgAl_2O_4 + CuO \leftrightarrow CuAl_2O_4 + MgO \quad (5)$$

The presence of MgO indicated that some copper aluminate could have been formed during operation, although the phase $CuAl_2O_4$ is undistinguished of the $MgAl_2O_4$ phase by XRD analysis.

As it can be seen, similar crystallite compounds to the fresh OCs particles were detected in the correspoding used samples. This fact revealed that the attrited material is composed both of copper compounds and of support.

A possible cause of the high attrition found in Cu-γAl and Cu-αAl OCs, could be the formation of a new phase ($CuAlO_2$) found in used samples, both in oxidized and reduced samples. The formation of this copper aluminate in air atmosphere is favoured as temperature increases [37]. However, it is unstable at temperatures below 1273 K, and may decompose by the following chemical reactions [38]:

$$8CuAlO_2 + O_2 \rightarrow 4CuAl_2O_4 + 2\,Cu_2O \qquad (6)$$

$$4CuAlO_2 + O_2 \rightarrow 2CuAl_2O_4 + 2\,CuO \qquad (7)$$

Moreover, this copper aluminate was not previously detected in samples after 100 h of operation in a 10 kW_{th} unit operated at lower temperatures (T_{FR} = 1073 K and T_{AR} = 1073 K) using a CuO-γAl_2O_3 OC [34]. Therefore, the formation and dissociation of this metastable compound in particles operated at high temperature might increase the attrition of the particles.

Temperature-programmed reduction. The identification of the formation of $NiAl_2O_4$ in the fresh and after used Cu-NiAl particles should be carried out by TPR analysis due to XRD technique only detects crystalline phases with a content higher of 5 %. Therefore, TPR analyses of fresh and used particles of the different OCs were performed to determine the reducible species and the temperature at which the reduction of these species occurs. Figure 9 shows the different TPR profiles measured for the fresh and after used OCs particles. The TPR spectra showed several H_2 consumption peaks. The peak in the temperature range of 473–573 K is attributed to the reduction of dispersed and bulk CuO species [39]. The peak in the temperature range of 623–773 K is attributed to the reduction of $CuAl_2O_4$ [39]. The reduction of $CuAlO_2$ phase has a high temperature peak around 1033 K [36]. The high temperature peak at 1073–1273 K is associated with the reduction of Ni^{2+} in $NiAl_2O_4$ [40] .

Similar profiles were measured for the different OCs both fresh and after used. Fresh OCs presented a main peak corresponding to the reduction of CuO compound. After used OCs presented two main peaks attributed to CuO and $CuAl_2O_4$ reductions and a minor peak around 973 K corresponding to $CuAlO_2$ phase [36]. In this sense, TPR profiles are consistent with XRD data which indicate the presence of both CuO and $CuAl_2O_4$ as main phases in most of the samples and a minor existence of $CuAlO_2$ compound. The presence of $NiAl_2O_4$ in the Cu-NiAl OC was revealed by the high temperature peak characteristic of the reduction of this phase in both fresh and after-used particles. The chemical pre-treatment of the γAl_2O_3 with NiO to form partially the stable $NiAl_2O_4$ structure in the Cu-

NiAl OC could help to increase the temperature resistance of the particles and to reduce the attrition rate of this OC.

SEM-EDX analysis. Samples of the different OCs extracted from the AR at different operation times were also analyzed by SEM to determine changes produced in the structure of the solid materials during operation. Moreover, some particles were embedded in resin, cut, polished and analyzed by EDX. Images of cross sections of fresh and after used particles at the different tests and operation times are shown in Figure 10. Fresh particles exhibited an outer shell of CuO, specially Cu-γAl and Cu-MgAl OCs. However, this layer had disappeared after a few hours of operations due to attrition during operation. This fact was confirmed by EDX analysis and agreed with the CuO loss measured in after-used particles (see Table 3).

SEM analysis showed important structural changes for Cu-γAl, Cu-αAl, and Cu-MgAl OCs. An increase in the CuO grain size can be observed in these OCs, being especially important for Cu-MgAl OC. This copper sinterization could be due to operation at high temperature (T_{FR} = 1173 K, T_{AR} = 1223 K). Moreover, Cu-γAl and Cu-αAl particles experienced considerable degradation and have started to break apart through the crack formation around 20 h of operation. Although the exact mechanism of formation of these structural defects is unidentified, the sintering of copper and the formation of the metastable $CuAlO_2$ compound could help to chunk the particles.

SEM images confirm that the Cu-NiAl particles maintain their structural integrity and original homogeneity after more than 67 h of operation at high temperatures. The EDX analysis revealed the uniform distribution of Al, Cu and Ni inside the particles. The presence of $NiAl_2O_4$ in the Cu-NiAl OC structure could help to avoid the sintering process of Cu inside the particles and to reduce the attrition rate of this OC.

4. Discussion

The design of a CLC industrial unit must consider both operational and environmental aspects regarding to the selection of the oxygen carrier. According to the experimental work herein carried out, all Cu-based OCs developed can be used at T_{FR}=1173 K and T_{AR}=1223 K without agglomeration problems or deactivation of the carrier with a complete combustion of the fuel working at oxygen carrier to fuel ratios above ≈1.2, which corresponds to a solid circulation rate of ≈4.0 kg s^{-1} per MW_{th}. Being the maximum circulation rate of solids about 16 kg s^{-1} per MW_{th} [41], the optimal operation conditions ($\phi > 1.2$) could be easily reached in an industrial CLC system using Cu-based oxygen carriers.

From the operational point of view, in a CLC process an increase in the oxidation temperature boost the inlet gas temperature in the turbine, improving in this way the net plant efficiency. According to the experimental results, the OC prepared using $NiO/\gamma Al_2O_3$ as support can be used at T_{FR}=1173 K and T_{AR}=1223 K without any operational problems. Operational cost related with the oxygen carrier renovation should

be taking into account. High attrition rates will decrease the particle lifetime increasing the cost of the CLC process. Table 4 shows the number of the replacement times by year necessary for the different OCs. This value was calculated from the particle lifetime corresponding to the final value of the attrition rate measured at the operation conditions used in this work. The values obtained in previous works with the CuO-γAl_2O_3 OC after 100 h of operation in a 10 kW_{th} unit operated at lower temperatures (T_{FR} = 1073 K and T_{AR} = 1073 K) and after 63 h of operation in a 500 W_{th} at high AR temperature (T_{FR} = 1073 K and T_{AR} = 1173 K) have been included for comparison purposes [27, 34]. It can be seen that Cu-NiAl OC had a low attrition rate and the highest particle lifetime (2700 h) even working at high temperatures. As can be inferred from these results, an increase of 100 K in the T_{FR} and 150 K in T_{AR} can be done with the same replacement of the material that working at 1073 K in both reactors with the CuO-γAl_2O_3 OC.

In addition, Cu-based OC have always been rejected as best candidate for the CLC process due to its agglomeration problems and its restricted operational temperatures. The results found in this work show that Cu-based OC can be used at higher temperatures than referred before without any operational problems. This is the first time that a Cu-based OC, prepared by a commercial manufacturing method, and used at 1173K in the FR and 1223 K in the AR exhibits such a good properties (high reactivity together with high mechanical durability and absence of agglomeration). This result opens new possibilities for the application of Cu-based materials in industrial-scale CLC processes.

Nevertheless, the OC developed in this work with high temperature resistance contains a low amount of NiO (3 wt.%). Some drawbacks are derived from this NiO content, an expensive metal oxide with important health and environmental hazards. By the one hand, the use of NiO, more expensive than CuO, would increase the costs of the oxygen carrier manufacture. By the other hand, it would be necessary a waste management analysis of this OC due to the environmental risks of Ni. Although in a previous work [17], it was found that the solid waste generated in a CLC process working with CuO-γAl_2O_3 OC can be classified as a stable nonreactive hazardous waste acceptable at landfills for nonhazardous wastes, the presence of a small fraction of NiO or $NiAl_2O_4$ in the residue would required more detailed studies.

5. Conclusions

Several Cu-based oxygen carriers have been developed by impregnation on different supports (γAl_2O_3, αAl_2O_3, $MgAl_2O_4$, and NiO/γAl_2O_3). The supports were prepared by thermal or chemical modifications of commercial γAl_2O_3 with the aim of reduce the interaction with the metal oxide. The influence of the support on the high temperature behaviour of the different Cu-based oxygen carriers was analyzed during long-term test in a 500 W_{th} CLC unit under continuous operation using methane as fuel and high temperatures both in FR, 1173 K and in AR, 1223 K. The behaviour of the different OCs on the process performance was evaluated taking into account important aspects such as: combustion efficiency, resistance to attrition, fluidization behaviour (no presence of agglomeration) and maintenance of the oxygen-carrying capacity and reactivity. A total

of 209 h in hot conditions were carried out, of which 176 h corresponded at combustion conditions with methane.

Complete fuel combustion was reached at $\phi > 1.2$ with all OCs. Moreover, in spite of the high temperatures used in the tests, agglomeration or defluidization of the bed were never detected in reducing or oxidation conditions with any of the OCs used in this work.

Cu-γAl and Cu-αAl OCs had an abrupt increase of the attrition rate resembling that the particles had chunked and Cu-MgAl OC had a high attrition rate. On the other hand, Cu-NiAl OC had a low and stable attrition rate after 67 h of operation at high temperature, maintaining its structural integrity and original homogeneity. The presence of $NiAl_2O_4$ in the Cu-NiAl OC structure could help to avoid the sintering process of Cu inside the particles and to reduce the attrition rate of this OC. It was concluded that a Cu-based OC prepared using γAl_2O_3 as support modified with a small NiO addition is adequate to operate without attrition or agglomeration problems in the CLC process at high temperature.

This is the first time that a Cu-based OC, prepared by a commercial manufacturing method, and used at 1173K in the FR and 1223 K in the AR exhibits such a good properties: high reactivity together with high mechanical durability and absence of agglomeration. This result opens new possibilities for the application of Cu-based materials in industrial-scale CLC processes.

Acknowledgements

This research was conducted with financial support from the Spanish Ministry of Science and Innovation (MICINN, Project CTQ2007-64400) and C.S.I.C. (200480E619).

Tables

Table 1. Properties of the fresh Cu-based OCs.

Table 2. Experimental conditions of the long-term tests in the CLC continuous unit of 500 W_{th}.

Table 3. Properties of the after used Cu-based OCs.

Table 4. Summary of the particle lifetime and the replacement times/ year for different OCs at different operating temperatures.

Table 1. Properties of the fresh Cu-based OCs.

	Cu-γAl	**Cu-αAl**	**Cu-MgAl**	**Cu-NiAl**
CuO content (wt%)	14.2	15	12	12.8
Oxygen transport capacity $R_{o,OC}$ (%)	2.86	3.02	2.41	2.57[a]
Particle size (μm)	300-500	300-500	300-500	300-500
Porosity (%)	50	45	40	54
Specific surface area BET (m^2/g)	91.3	6.8	53	91.4
Bulk density (g/cm^3)	1.7	2.2	1.9	1.6
Crushing strength (N)	2.9	4.6	2.1	3.1
Crystalline phases	CuO	CuO	CuO	CuO
	$CuAl_2O_4$	$CuAl_2O_4$[b]		$CuAl_2O_4$
			$MgAl_2O_4$	$NiAl_2O_4$[b, c]
	γAl_2O_3	αAl_2O_3		γAl_2O_3

[a] NiO as inert. [b] Minor amount [c] Identified by TPR

Table 2. Experimental conditions of the long-term tests in the CLC continuous unit of 500 Wth.

Oxygen carrier	T_{FR} (K)	T_{AR} (K)	ϕ	CH_4 [a] (%)	$t_{combustion}$ (h)
Cu-γAl	1173	1223	1.0 - 1.4	25 - 35	29
Cu-αAl	1173	1223	1.0 - 1.4	20 - 30	30
Cu-MgAl	1173	1223	1.0 - 1.4	20 - 30	50
Cu-NiAl	1173	1223	1.0 - 1.5	20 - 30	67

[a] N_2 was used for balance

Table 3. Properties of the after used Cu-based OCs.

OC	**Cu-γAl**	**Cu-αAl**	**Cu-MgAl**	**Cu-NiAl**
Operation time	**29 h**	**30 h**	**50 h**	**67 h**
CuO content (wt %)	13	12.6	8.5	10.6
Oxygen transport capacity $R_{o,OC}$ (%)	2.62	2.53	1.71	2.13 [a]
Porosity (%)	58	49	43	41
Specific surface area BET (m^2/g)	6.8	2.9	4.9	4.9
Bulk density (g/cm^3)	1.5	2.0	2.0	2.1
Crushing strength (N)	0.6	1.8	1.7	2.0
Crystalline phases, particles from AR	CuO	CuO	CuO	CuO
	$CuAl_2O_4$	$CuAl_2O_4$		$CuAl_2O_4$
			MgO	$NiAl_2O_4$ [b]
	αAl_2O_3	αAl_2O_3	$MgAl_2O_4$	αAl_2O_3
Crystalline phases, particles from FR filter	Cu	Cu	Cu	Cu
	CuO	CuO	CuO	CuO
	Cu_2O	Cu_2O	Cu_2O	Cu_2O

	$CuAl_2O_4$	$CuAl_2O_4$		$CuAl_2O_4$
		$CuAlO_2$		
	αAl_2O_3	αAl_2O_3	$MgAl_2O_4$	αAl_2O_3
Crystalline phases, particles from AR filter	CuO	CuO	CuO	CuO
				$CuAl_2O_4$
	$CuAl_2O_4$	$CuAl_2O_4$		
	$CuAlO_2$	$CuAlO_2$		$NiAl_2O_4$[b]
			$MgAl_2O_4$	αAl_2O_3
	αAl_2O_3	αAl_2O_3		

[a] NiO as inert. [b] Identified by TPR

Table 4. Summary of the particle lifetime and the replacement times/year for different OCs at different operating temperatures.

	Cu-γAl[a]	**Cu-γAl[b]**	**Cu-MgAl**	**Cu-NiAl**
Temperatures FR – AR	1073-1073	1073-1173	1173-1223	1173-1223
$t_{combustion}$ (h)	100	63	50	67
Attrition rate (%/h)	0.04	0.09	0.20	0.04
Particle lifetime (h)	2500	1100	500	2700
Replacement times / year [c]	3.4	7.8	17.3	3.2

[a] de Diego et al., 2007 [34] [b] Forero et al., 2010 [27] [c] n=8640/particle lifetime

Figure captions

Figure 1. Schematic diagram of the Chemical-Looping Combustion continuous unit of 500 Wth.

Figure 2. Effect of the oxygen carrier to fuel ratio on the combustion efficiency for the different OCs. T_{FR}= 1173 K ,T_{AR}= 1223 K.

Figure 3. SEM micrograph pictures of after-used particles for the different Cu-based OCs.

Figure 4. Attrition rates vs. time of the different Cu-based OCs. T_{FR}= 1173 K, T_{AR}= 1223 K.

Figure 5. CuO content vs. time curves of the different Cu-based OCs. T_{FR}= 1173 K, T_{AR}= 1223 K.

Figure 6. Solid conversion vs. time curves in TGA for a) reduction and b) oxidation reactions of fresh and after-used Cu-based OCs particles. Reduction: CH_4 = 15%, H_2O = 20%, N_2 = 65%. Oxidation: air. T=1073 K

Figure 7. Pore size distributions of a) fresh and b) after-used Cu-based OCs .

Figure 8. Crushing strength evolution of the different Cu-based OCs.

Figure 9. H_2-TPR profiles of the fresh and after-used Cu-based OCs.

Figure 10. SEM pictures of cross sections of fresh and after-used particles at different operation times for the Cu-based OCs.

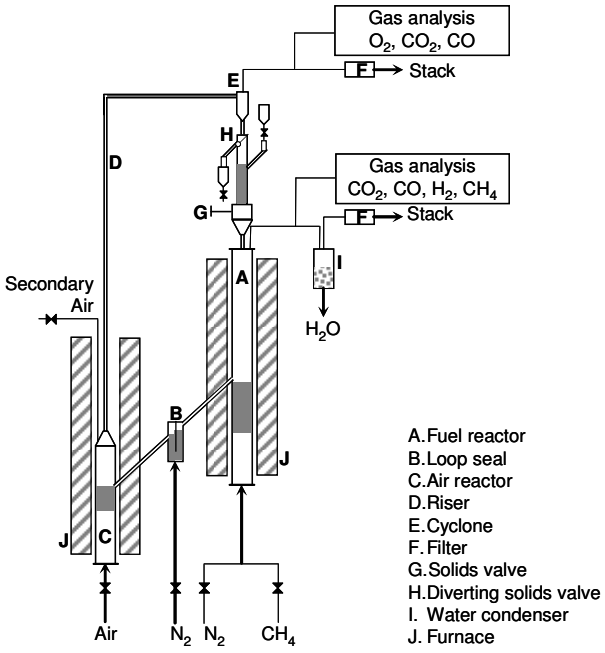

Figure 1. Schematic diagram of the Chemical-Looping Combustion continuous unit of 500 Wth.

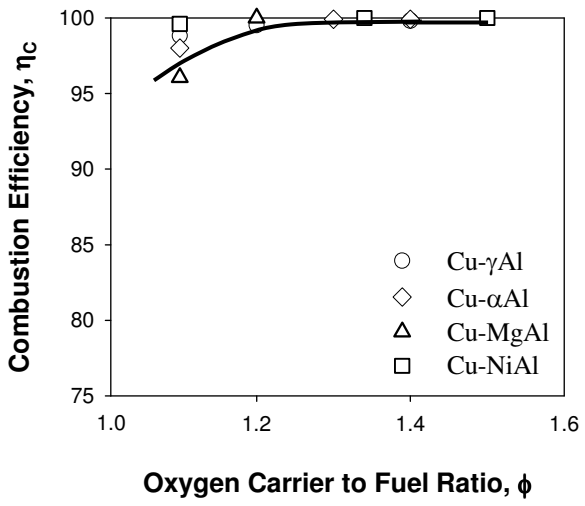

Figure 2. Effect of the oxygen carrier to fuel ratio on the combustion efficiency for the different OCs. T_{FR}= 1173 K ,T_{AR}= 1223 K.

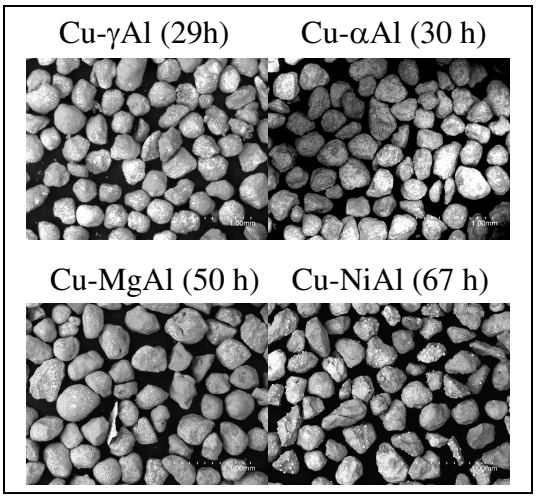

Figure 3. SEM micrograph pictures of after-used particles for the different Cu-based OCs.

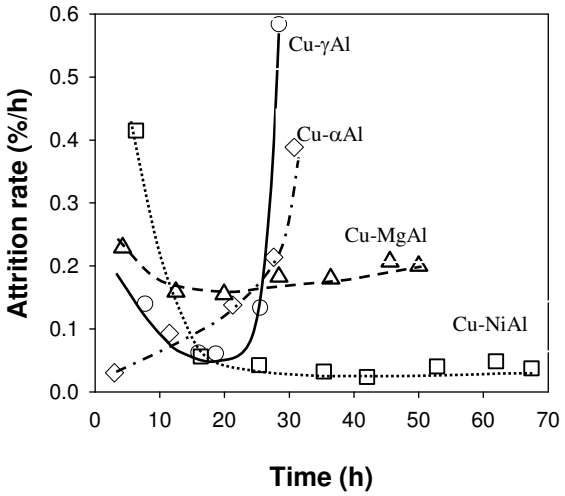

Figure 4. Attrition rates vs. time of the different Cu-based OCs. T_{FR}= 1173 K, T_{AR}= 1223 K.

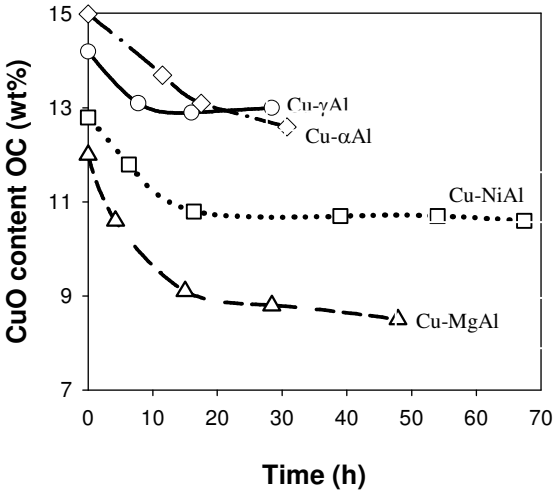

Figure 5. CuO content vs. time curves of the different Cu-based OCs. T_{FR}= 1173 K, T_{AR}= 1223 K.

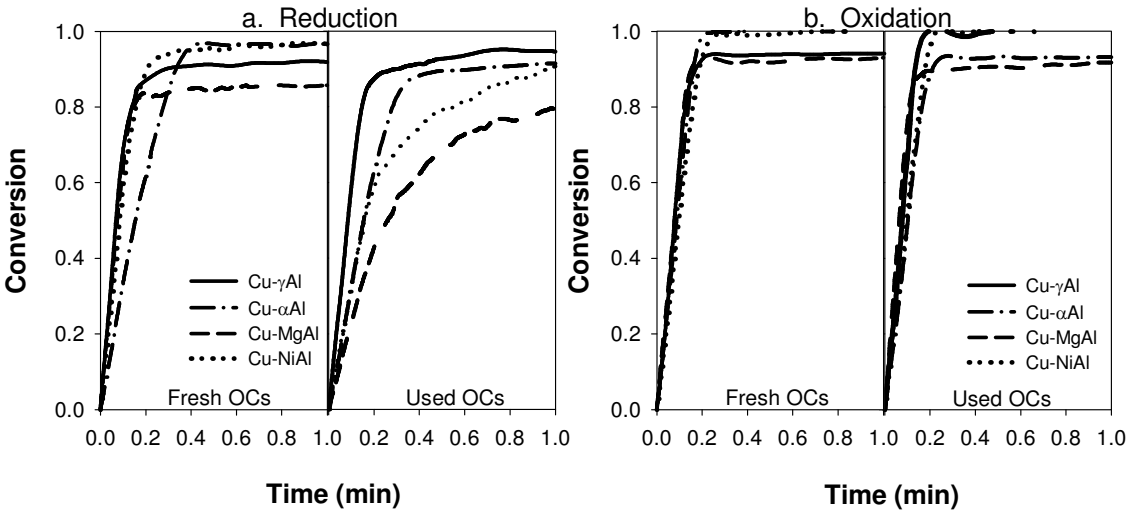

Figure 6. Solid conversion vs. time curves in TGA for a) reduction and b) oxidation reactions of fresh and after-used Cu-based OCs particles. Reduction: CH_4 = 15%, H_2O = 20%, N_2 = 65%. Oxidation: air. T=1073 K

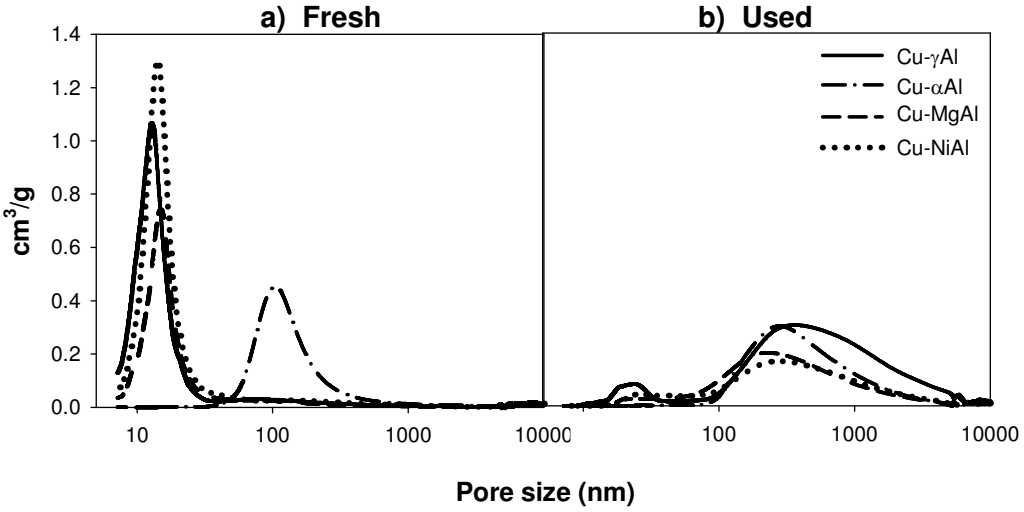

Figure 7. Pore size distributions of a) fresh and b) after-used Cu-based OCs.

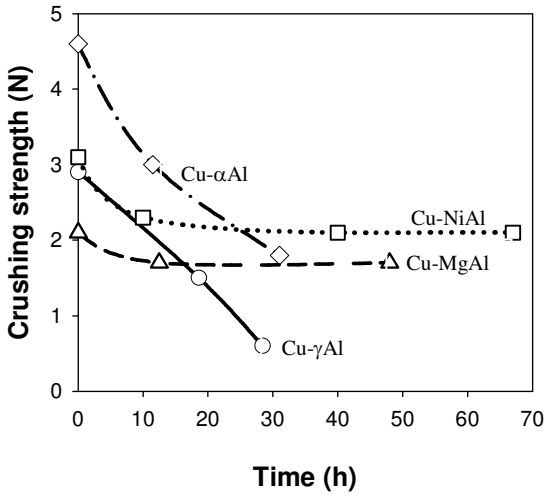

Figure 8. Crushing strength evolution of the different Cu-based OCs.

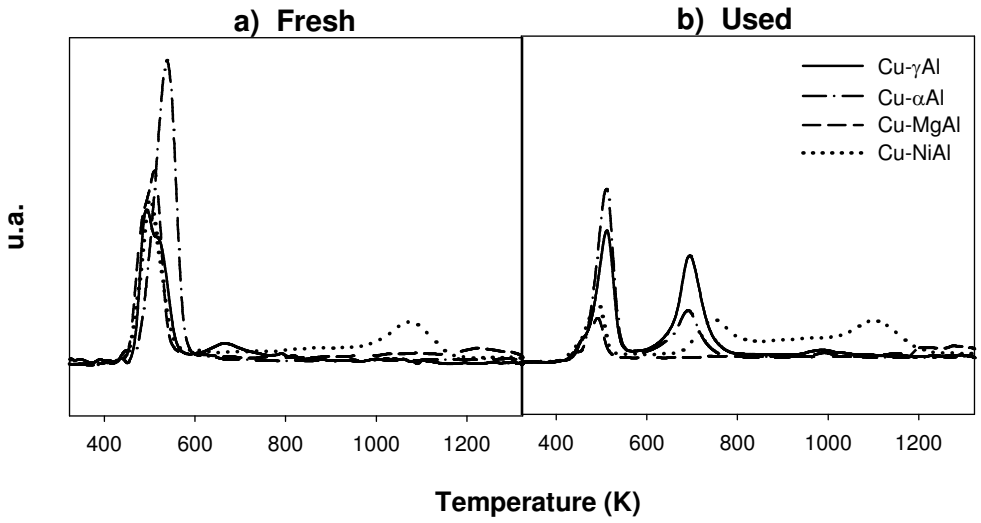

Figure 9. H_2-TPR profiles of the fresh and after-used Cu-based OCs.

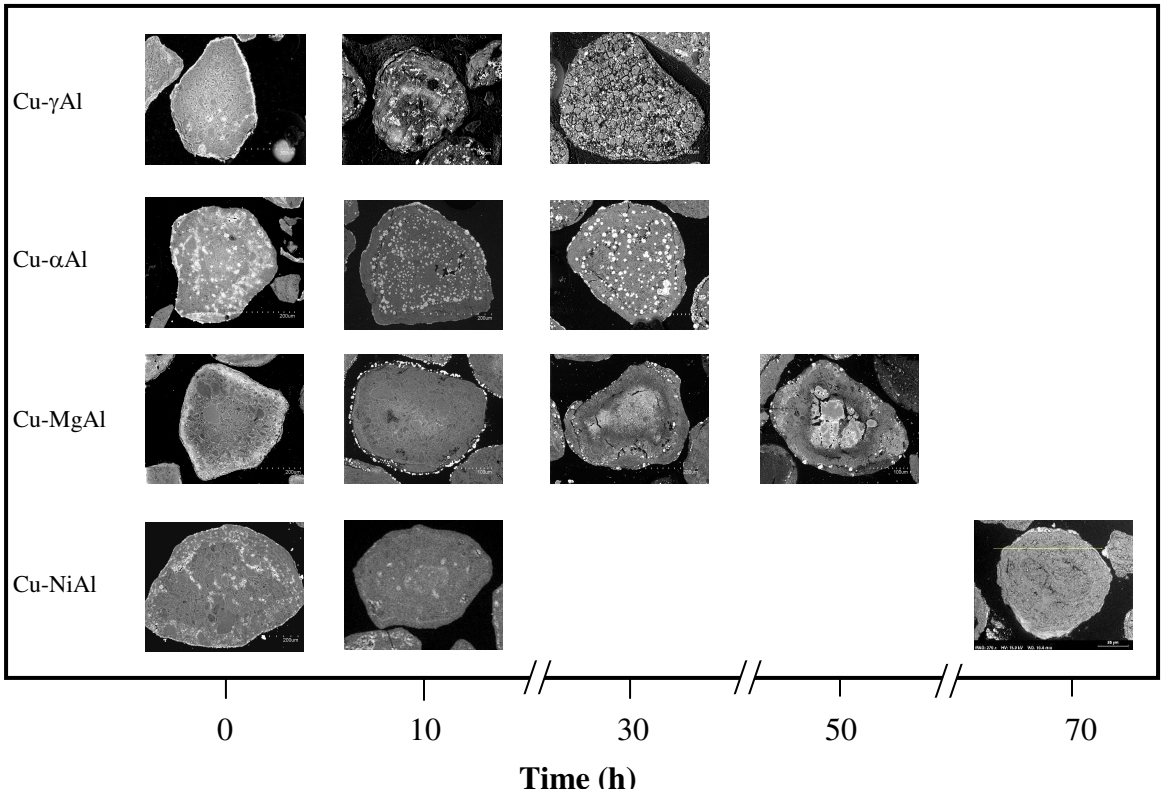

Figure 10. SEM pictures of cross sections of fresh and after-used particles at different operation times for the Cu-based OCs.

REFERENCES

1. IPCC, *Cambio climático 2007: Informe de síntesis. Contribución de los grupos de trabajo I, II y III al cuarto informe de evaluación del grupo intergubernamental de expertos sobre el cambio climático*. [Equipo de redacción principal: Pachauri, R.K. y Reisinger, A. (directores de la publicación)]: Ginebra, Suiza, 104 págs, 2007.
2. Kerr, H. R., Capture and separation technology gaps and priority research needs. In *Carbon Dioxide Capture for Storage in Deep Geologic Formations-Results from the CO_2 Capture Project*, Thomas, D.; Benson, S., Eds. Elsevier Science: Amsterdam, 2005; Vol. 1, pp 655-660 (Chapter 38).
3. Kvamsdal, H. M.; Jordal, K.; Bolland, O., A quantitative comparison of gas turbine cycles with CO_2 capture. *Energy* **2007,** 32, (1), 10-24.
4. Linderholm, C.; Abad, A.; Mattisson, T.; Lyngfelt, A., 160 h of chemical-looping combustion in a 10 kW reactor system with a NiO-based oxygen carrier. *International Journal of Greenhouse Gas Control* **2008,** 2, (4), 520-530.
5. Kolbitsch, P.; Bolhàr-Nordenkampf, J.; Pröll, T.; Hofbauer, H., Comparison of two Ni-based oxygen carriers for chemical looping combustion of natural gas in 140 kW continuous looping operation. *Industrial & Engineering Chemistry Research* **2009,** 48, (11), 5542-5547.
6. Adánez, J.; Gayán, P.; Celaya, J.; de Diego, L. F.; García-Labiano, F.; Abad, A., Chemical looping combustion in a 10 kW_{th} prototype using a CuO/Al_2O_3 oxygen carrier: Effect of operating conditions on methane combustion. *Industrial and Engineering Chemistry Research* **2006,** 45, (17), 6075-6080.
7. Ryu, H.-J.; Jin, G.-T.; Yi, C.-K.; Rubin, E. S.; Keith, D. W.; Gilboy, C. F.; Wilson, M.; Morris, T.; Gale, J.; Thambimuthu, K., Demonstration of inherent CO_2 separation and no NOx emission in a 50kW chemical-looping combustor: Continuous reduction and oxidation experiment. In *Greenhouse Gas Control Technologies 7*, Elsevier Science Ltd: Oxford, 2005; pp 1907-1910.
8. Lyngfelt, A.; Thunman, H., Construction and 100 h of operational experience of a 10-kW chemical-looping combustor. In *Carbon Dioxide Capture for Storage in Deep Geologic Formations-Results from the CO_2 Capture Project*, Thomas, D.; Benson, S., Eds. Elsevier Science: Amsterdam, 2005; Vol. 1, pp 625-645 (Chapter 36).
9. Kolbitsch, P.; Pröll, T.; Bolhàr-Nordenkampf, J.; Hofbauer, H., Operating experience with chemical looping combustion in a 120 kW dual circulating fluidized bed (DCFB) unit. *Energy Procedia* **2009,** 1, (1), 1465-1472.
10. Adánez, J.; de Diego, L. F.; García-Labiano, F.; Gayán, P.; Abad, A.; Palacios, J. M., Selection of oxygen carriers for chemical-looping combustion. *Energy and Fuels* **2004,** 18, (2), 371-377.
11. Copeland, R. J.; Alptekin, G.; Cesario, M.; Gershanovich, Y. In *Sorbent energy transfer system (SETS) for CO_2 separation with high efficiency*, 27th International Technical Conference on Coal Utilization & Fuel Systems, CTA: Clearwater, Florida, USA, March 4-7,, 2002; Florida, USA, 2002; pp 719-729.
12. Chuang, S. Y.; Dennis, J. S.; Hayhurst, A. N.; Scott, S. A., Development and performance of Cu-based oxygen carriers for chemical-looping combustion. *Combustion and Flame* **2008,** 154, (1-2), 109-121.
13. Johansson, M.; Mattisson, T.; Lyngfelt, A. In *Comparison of oxygen carriers for chemical-looping combustion of methane-rich fuels*, 19th International Conference on Fluidized Bed Combustion, Vienna, Austria, May 21-24, 2006, 2006; Vienna, Austria, 2006.
14. Son, S. R.; Go, K. S.; Kim, S. D., Thermogravimetric analysis of copper oxide for chemical-looping hydrogen generation. *Industrial & Engineering Chemistry Research* **2009,** 48, (1), 380-387.
15. de Diego, L. F.; García-Labiano, F.; Adánez, J.; Gayán, P.; Abad, A.; Corbella, B. M.; Palacios, J. M., Development of Cu-based oxygen carriers for chemical-looping combustion. *Fuel* **2004,** 83, (13), 1749-1757.
16. de Diego, L. F.; Gayán, P.; García-Labiano, F.; Celaya, J.; Abad, A.; Adánez, J., Impregnated CuO/Al_2O_3 oxygen carriers for chemical-looping combustion: Avoiding fluidized bed agglomeration. *Energy and Fuels* **2005,** 19, (5), 1850-1856.

17. García-Labiano, F.; Gayán, P.; Adánez, J.; de Diego, L. F.; Forero, C. R., Solid waste management of a chemical-looping combustion plant using Cu-based oxygen carriers. *Environmental Science and Technology* **2007,** 41, (16), 5882-5887.
18. Forero, C. R.; Gayán, P.; de Diego, L. F.; Abad, A.; García-Labiano, F.; Adánez, J., Syngas combustion in a 500 W_{th} chemical-looping combustion system using an impregnated Cu-based oxygen carrier. *Fuel Processing Technology* **2009,** 90, (12), 1471-1479.
19. Gayán, P.; Forero, C. R.; de Diego, L. F.; Abad, A.; García-Labiano, F.; Adánez, J., Effect of gas composition in chemical-looping combustion with copper-based oxygen carriers: fate of light hydrocarbons. *International Journal of Greenhouse Gas Control* **2010,** 4, (1), 13-22.
20. Forero, C. R.; Gayán, P.; García-Labiano, F.; de Diego, L. F.; Abad, A.; Adánez, J., Effect of gas composition in chemical-looping combustion with copper-based oxygen carriers: fate of sulphur. *International Journal of Greenhouse Gas Control* **2010,** 4, (5), 762-770.
21. Yu, J.; Corripio, A. B.; Harrison, D. P.; Copeland, R. J., Analysis of the sorbent energy transfer system (SETS) for power generation and CO_2 capture. *Advances in Environmental Research* **2003,** 7, (2), 335-345.
22. Wolf, J.; Yan, J., Parametric study of chemical looping combustion for tri-generation of hydrogen, heat, and electrical power with CO_2 capture. *International Journal of Energy Research* **2005,** 29, (8), 739-753.
23. Jin, H.; Ishida, M., Investigation of a novel gas turbine cycle with coal gas fueled chemical-looping combustion. *American Society of Mechanical Engineers, Advanced Energy Systems Division (Publication) AES* **2000,** 40, 547-552.
24. Anheden, M.; Svedberg, G. In *Chemical-looping combustion in combination with integrated coal gasification.*, 31st Intersociety Energy Conversion Engineering Conference - IECEC, Washington D.C. (IEEE) 1996; Washington D.C. (IEEE) 1996; pp 2045-2050.
25. Naqvi, R.; Bolland, O., Multi-stage chemical looping combustion (CLC) for combined cycles with CO_2 capture. *International Journal of Greenhouse Gas Control* **2007,** 1, (1), 19-30.
26. Cho, P.; Mattisson, T.; Lyngfelt, A., Comparison of iron-, nickel-, copper- and manganese-based oxygen carriers for chemical-looping combustion. *Fuel* **2004,** 83, (9), 1215-1225.
27. Forero, C. R.; Gayán, P.; García-Labiano, F.; de Diego, L. F.; Abad, A.; Adánez, J., High temperature behaviour of a $CuO/\gamma Al_2O_3$ oxygen carrier for chemical-looping combustion. *Submit for publication in International Journal of Grenhouse Gas Control* **2010**.
28. Gayán, P.; de Diego, L. F.; García-Labiano, F.; Adánez, J.; Abad, A.; Dueso, C., Effect of support on reactivity and selectivity of Ni-based oxygen carriers for chemical-looping combustion. *Fuel* **2008,** 87, (12), 2641-2650.
29. Singh, V. K.; Sinha, R. K., Low temperature synthesis of spinel ($MgAl_2O_4$). *Materials Letters* **1997,** 31, (3-6), 281-285.
30. Zafar, Q.; Mattisson, T.; Gevert, B., Redox investigation of some oxides of transition-state metals Ni, Cu, Fe, and supported on SiO_2 and $MgAl_2O_4$. *Energy and Fuels* **2006,** 20, (1), 34-44.
31. Adánez, J.; García-Labiano, F.; De Diego, L. F.; Gayán, P.; Celaya, J.; Abad, A., Nickel-copper oxygen carriers to reach zero CO and H_2 emissions in chemical-looping combustion. *Industrial and Engineering Chemistry Research* **2006,** 45, (8), 2617-2625.
32. García-Labiano, F.; de Diego, L. F.; Adánez, J.; Abad, A.; Gayán, P., Reduction and oxidation kinetics of a copper-based oxygen carrier prepared by impregnation for chemical-looping combustion. *Industrial and Engineering Chemistry Research* **2004,** 43, (26), 8168-8177.
33. Lyngfelt, A.; Kronberger, B.; Adánez, J.; Morin, J. X.; Hurst, P.; Rubin, E. S.; Keith, D. W.; Gilboy, C. F.; Wilson, M.; Morris, T.; Gale, J.; Thambimuthu, K., The grace project: Development of oxygen carrier particles for chemical-looping combustion. Design and operation of a 10 kW chemical-looping combustor. In *Greenhouse Gas Control Technologies 7*, Elsevier Science Ltd: Oxford, 2005; pp 115-123.
34. de Diego, L. F.; García-Labiano, F.; Gayán, P.; Celaya, J.; Palacios, J. M.; Adánez, J., Operation of a 10 kW_{th} chemical-looping combustor during 200 h with a $CuO-Al_2O_3$ oxygen carrier. *Fuel* **2007,** 86, (7-8), 1036-1045.
35. Johansson, M.; Mattisson, T.; Lyngfelt, A., Investigation of Fe_2O_3 with $MgAl_2O_4$ for chemical-looping combustion. *Industrial and Engineering Chemistry Research* **2004,** 43, (22), 6978-6987.

36. Artizzu, P.; Garbowski, E.; Primet, M.; Brulle, Y.; Saint-Just, J., Catalytic combustion of methane on aluminate-supported copper oxide. *Catalysis Today* **1999,** 47, (1-4), 83-93.
37. Bolt, P. H.; Habraken, F. H. P. M.; Geus, J. W., Formation of nickel, cobalt, copper, and iron aluminates from α - and γ-alumina-supported oxides: A comparative study. *Journal of Solid State Chemistry* **1998,** 135, (1), 59-69.
38. Susnitzky, D.; Carter, B., The formation of copper aluminate by solid-state reaction. *J. Mater. Res.* **1991,** 6, 1958-1963.
39. Luo, M.-F.; Fang, P.; He, M.; Xie, Y.-L., In situ XRD, Raman, and TPR studies of CuO/Al_2O_3 catalysts for CO oxidation. *Journal of Molecular Catalysis A: Chemical* **2005,** 239, (1-2), 243-248.
40. Li, C.; Chen, Y.-W., Temperature-programmed-reduction studies of nickel oxide/alumina catalysts: effects of the preparation method. *Thermochimica Acta* **1995,** 256, (2), 457-465.
41. Abad, A.; Adánez, J.; García-Labiano, F.; de Diego, L. F.; Gayán, P.; Celaya, J., Mapping of the range of operational conditions for Cu-, Fe-, and Ni-based oxygen carriers in chemical-looping combustion. *Chemical Engineering Science* **2007,** 62, (1-2), 533-549.